

Article

# A New Plasma Surface Alloying to Improve the Wear Resistance of the Metallic Card Clothing

Dongbo Wei <sup>1,2,\*</sup> , Fengkun Li <sup>1,\*</sup>, Shuqin Li <sup>1</sup>, Xiaohu Chen <sup>1</sup>, Feng Ding <sup>1</sup>, Pingze Zhang <sup>1,3</sup> and Zhangzhong Wang <sup>3</sup>

<sup>1</sup> College of Materials Science and Technology, Nanjing University of Aeronautics and Astronautics, Nanjing 211106, China; shuqli@nuaa.edu.cn (S.L.); chenxiaohu@nuaa.edu.cn (X.C.); dingf@nuaa.edu.cn (F.D.); zhangpingze@nuaa.edu.cn (P.Z.)

<sup>2</sup> Key Laboratory of Materials Preparation and Protection for Harsh Environment (Nanjing University of Aeronautics and Astronautics), Ministry of Industry and Information Technology, Nanjing 211106, China

<sup>3</sup> Jiangsu Key Laboratory of Advanced Structural Materials and Application Technology, Nanjing 211167, China; zzww@njit.edu.cn

\* Correspondence: weidongbo@nuaa.edu.cn (D.W.); lifengkun@nuaa.edu.cn (F.L.)

Received: 3 April 2019; Accepted: 28 April 2019; Published: 6 May 2019



**Abstract:** A new surface strengthening process: Plasma surface chromizing was implemented on the metallic card clothing to improve its wear resistance based on double glow plasma surface metallurgy technology. A chromizing coating was prepared in the process, which consisted of a deposited layer and diffusion layer. The surface morphologies, microstructure, phase composition, and hardness were analyzed in detail. The friction behaviors of the metallic card clothing before and after plasma surface alloying were comparatively analyzed under various sliding speeds at room temperature. The results showed that: 1. The chromizing coating on the surface of metallic card clothing was dense and homogeneous without defects, and the metallic card clothing still maintained its integrity and sharpness. 2. The chromizing coating consist of [Fe,Cr], Cr, Cr<sub>23</sub>C<sub>6</sub>, and Cr<sub>7</sub>C<sub>3</sub>, which contribute to the high hardness. 3. The average microhardness of metallic card clothing increased from 365.4 HV<sub>0.05</sub> to 564.9 HV<sub>0.05</sub> after plasma surface chromizing. Nano hardness of the chromizing coating was approximately 1.87 times than the metallic card clothing. 4. At various sliding velocities of 2 m/min, 4 m/min, and 6 m/min, the specific wear rates of metallic card clothing were 16.38, 9.06 and 6.26 × 10<sup>-4</sup>·mm<sup>3</sup>·N<sup>-1</sup>·m<sup>-1</sup>, and the specific wear rates of metallic card clothing after plasma surface chromizing were 2.91, 3.30, and 2.95 × 10<sup>-4</sup>·mm<sup>3</sup>·N<sup>-1</sup>·m<sup>-1</sup>. Furthermore, the wear mechanism of the chromizing coating gradually changed from adhesive wear to abrasive wear as the sliding velocity increased. The results indicate that the wear resistance of metallic card clothing was improved obviously after plasma surface chromizing.

**Keywords:** the metallic card clothing; double glow plasma surface metallurgy technology; chromizing coating; wear resistance

## 1. Introduction

Textile industry occupies an important position in the national economy, and carding is an important process in textile production. As the main equipment of carding operation, carding machine plays an important role in textile production. At the same time, as the key part of carding machine, the main function of metallic card clothing is to comb and purify the fiber, and finally to remix the high-quality fiber. Additionally, the quality of metallic card clothing determines the quality of fiber significantly.

However, the poor wear resistance reduces the service life and carding quality of metallic card clothing. Through the high-speed contact friction and collision with all types of dust particles and

impurities being mixed with the cotton fiber, the metallic card clothing front and the tooth surface top are passivated. The wear occurs mainly on the upper part of the card wire teeth. The actual working angle on the tip of the wire teeth became high, causing the metallic card clothing to lose its fiber grip ability gradually and having tremendous effect on the carding quality [1]. In addition, during the high-speed friction, the friction heat effect could cause the metallic card clothing wires to reach a high temperature, which would lead to the metallic card clothing tip softening. The friction heat could be used to transform the abrasive grain wear into hard abrasive wear [2]. Both the temperature change and the thermal shock could also be the sources of surface fatigue, which lead to a fatigue failure [3].

Heat treatment has often been used for improving the hardness of the metallic card clothing so as to improve the wear resistance. Main heat treatment methods include spheroidizing annealing and quenching. The wear resistance of the metallic card clothing is improved after quenching. However, the heating parameters are unstable in the process of quenching, which can cause uneven microstructure. The higher content of carbon causes rapid rising of austenite grain after quenching. As the same time, martensitic carbon content will increase and more twins martensitic are formed during quenching, which is harmful to limit micro crack propagation [1,2]. Therefore, there exists some disadvantages in improving the anti-wear property of the metallic card clothing in the traditional heat treatment method.

Recently, certain new surface modification technologies have been utilized to improve the wear resistance of the materials. The double glow plasma surface metallurgy technology provided a new plasma strengthening process for the wear resistance improvement of the metallic card clothing. The double glow plasma surface metallurgy technology (referred to as “double glow technology”) is a new metal surface alloying technology, developed independently by Chinese scholars (Xu Zhong) on the basis of ion nitriding and sputtering. The schematic illustration and equipment drawing is presented in Figure 1. The anode-source electrode (target) and the anode-substrate electrode (substrate) formed two independently regulating discharge systems [4]. During experimentation, the chamber was vacuumed and the working gas (argon) was injected. When a pulsed DC power supply was switched on, a glow was generated between the anode and the source electrode, as well as between the anode and substrate electrode due to the plasma discharge. Simultaneously, the argon was ionized into argon ions. Under the electric field, the argon ions continuously bombarded the source and substrate electrodes. The constant bombardment of argon ions caused the cathode temperature to increase, reaching the pre-penetration temperature. The constant bombardment of argon ions caused the target to continuously splash target ions (M) [4]. Under the electric field, the target ions (M) were deposited on the substrate and diffused to the interior, forming an alloyed layer with specific properties [5]. The alloy layers are formed by the deposition and diffusion of the elements, whereas the corresponding composition and properties present a gradual distribution with depth, which demonstrated the metallurgical bonding characteristic. This structure could effectively improve the adhesion between the alloy layer and substrate. The double glow technology is widely utilized to improve the wear resistance, the corrosion resistance, the fatigue resistance, and the high temperature oxidation of metal materials [6–11]. Qiuzhongkai et al. prepared W-Mo coatings on the gear steel surfaced through the double plasma technology. The high resistance to plastic deformation and load-carrying capacity of the W-Mo coating could improve the gear steel wear resistance under both room and high temperatures (500 °C). The wear rate of the treated gear steel at room temperatures was only 19 percent of the untreated specimen wear rate [12]. Wei Cong et al. prepared Ni-Cr alloy layers on the low carbon steel surfaces through the double glow technology, which effectively reduces the low carbon steel wear rate under the normal temperatures [13]. In addition, compared with the traditional diffusion technology, the diffusion temperature in the process of double glow technology is lower, which will reduce the impact on the mechanical properties of the metallic card clothing and prevent its thermal deformation [14].

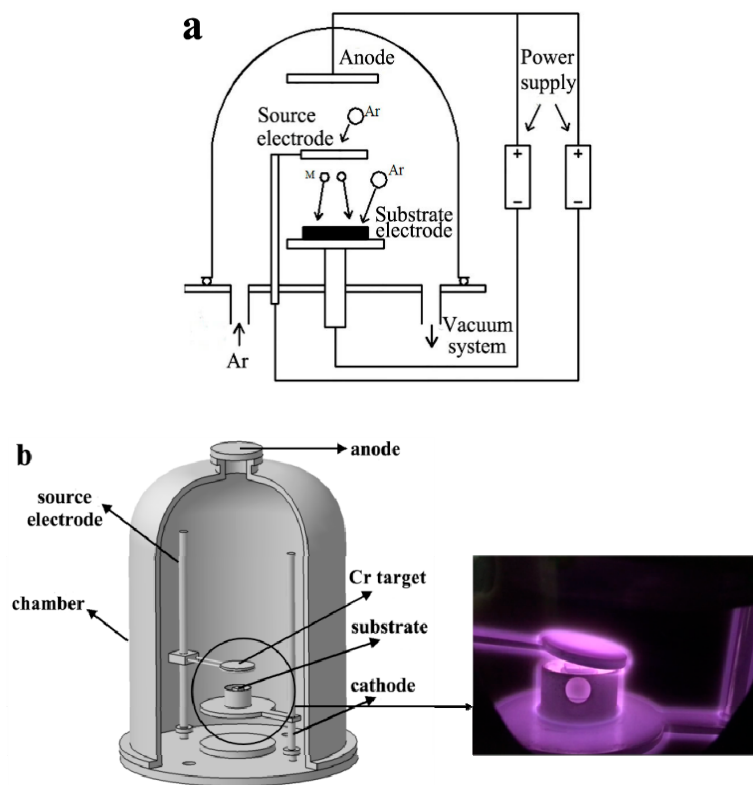


**Figure 1.** Schematic illustration (a) and equipment drawing (b) of double glow plasma technology.

Therefore, we used the new plasma surface strengthening process (double glow technology) to improve the wear resistance of the metallic card clothing. The chromizing coating was prepared on the metallic card clothing by double glow technology. The strengthening effects of the chromizing coating on the metallic card clothing were comparatively analyzed from the aspects of microstructure, hardness, elasticity modulus, and wear properties. The friction and wear behavior of the metallic card clothing before and after plasma surface alloying were carried out on a reciprocating sliding friction-wear tester with the Si<sub>3</sub>N<sub>4</sub> ball under various sliding speeds (2 m/min, 420 g; 4 m/min, 420 g; 6 m/min, 420 g) at room temperature.

## 2. Experimental Procedure

### 2.1. Preparation of Specimens

In the study, the metallic card clothing is made by 72B spring steel. Table 1 shows its chemical composition. Prior to the coating preparation, the substrate surface was polished with SiC emery papers (P180, P400, P600, P1000, and P1400). Following, acetone was utilized for ultrasonic cleaning and the samples were dried. ( $\Phi 100 \times 4 \text{ mm}^3$ , 99.95 wt.%, produced by Shenzhen Morgan Sputtering Target and Technology Co., Ltd., Shenzhen, China). The experimental parameters of the double glow technology are presented in Table 2.

**Table 1.** Chemical composition of 72B spring steel (wt.%).

Fe	C	Mn	Si	S	P
The rest	0.68–0.74	0.60–0.90	0.12–0.32	<0.025	<0.025

**Table 2.** Process parameters of double glow plasma treatment.

Parameter Influence Factors of Double Glow Plasma Treatment	Settings
distance between the source and substrate (mm)	20
voltage of the substrate (V)	450–480
electric current of the substrate (A)	1.1
voltage of the source (V)	900–960
electric current of the source (A)	1.7
soaking time (h)	3
working pressure (Pa)	35

### 2.2. Microstructure Analysis and Measurements

The microstructure and element distribution of the metallic card clothing after plasma surface alloying were characterized by scanning electron microscopy (SEM) and energy-dispersive X-ray spectrometry (EDS, produced by FEI Co. Ltd., Eindhoven, The Netherlands). A BrukerD8-ADVANCE diffractometer (Proto Manufacturing Inc., Oldcastle, ON, Canada) was used to determine the XRD (X-ray diffraction method) patterns of the chromizing coating using  $\text{CuK}\alpha 1$  radiation at 50 kV and 40 mA. Diffraction radiation were in a continuous mode with step size of  $0.02^\circ$  and step time of 8 s over the range of  $20^\circ < 2\theta < 90^\circ$ .

### 2.3. Strength Testing Methodologies

The surface microhardness of the metallic card clothing before and after plasma surface alloying was tested using HXS-100A microhardness tester (Ningbo yonghui instrument technology co. LTD, Ningbo, China) equipped with pyramid diamond indenter. There was a significant difference in the shape between the tip and the tooth body of metallic card clothing. Therefore, three different parts of each sample were selected as the test point, as shown in the Figure 2. The applied load was 50 g and loading time is 10 s. Each specimen is tested 5 points to get the arithmetic mean.

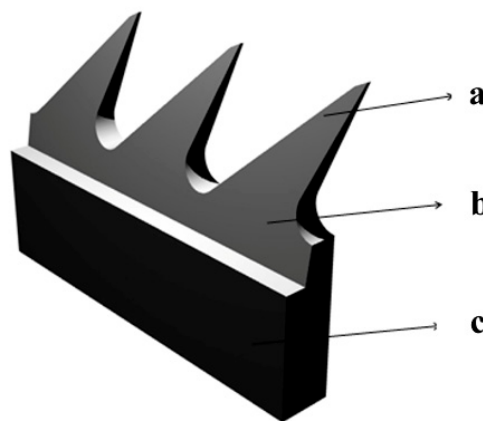


**Figure 2.** The schematic diagram of the test point. (a) The tooth point position of the metallic card clothing; (b) The position of the tooth base of the metal needle cloth; (c) The bottom of the metallic card clothing.

Nanoindentation tests were conducted with the Shimadzu dynamic microhardness tester (DUH-W201). The indenter was pressed onto the sample surface at the speed of  $1.3239 \text{ mN s}^{-1}$ ; the maximum load was 150 mN [12]. In order to avoid the substrate effect on the nanoindentation test, the maximum indentation depth should not exceed 10% of the coating thickness [15]. Three parallel experiments were conducted to improve the testing accuracy and the results were averaged.

## 2.4. Friction and Wear Test

At room temperature (relative humidity  $< 40 \pm 5\%$ ), the CET-I friction-wear tester with the  $\text{Si}_3\text{N}_4$  ball (hardness of 77 HRC (Rockwell hardness) and diameter of 3 mm) was utilized to conduct the dry wear sliding tests. For the friction tests, various sliding speeds (2 m/min, 420 g; 4 m/min, 420 g; 6 m/min, 420 g) were utilized, and the effects of different sliding speeds on the wear properties of metallic card clothing were studied. The wear test was described in the ASTM G133-05 standard [16]. During testing, the  $\text{Si}_3\text{N}_4$  ball produced reciprocating friction on the sample surfaces at various sliding speeds. The reciprocation length was 5 mm and the friction test duration was 10 min. After the friction test, the wear track profile was measured by the profilometer of the friction-wear tester. Three parallel experiments were conducted to improve the testing accuracy and the results were averaged. The schematic diagram of reciprocating friction (a), equipment drawing of CET-I friction-wear tester (b) and the schematic diagram of profilometer equipped by the friction-wear tester (c) are presented in Figure 3. The morphology of the wear track was analyzed through SEM. The weight loss comparison between the spring steel substrate and the alloy layers was inappropriate, because the densities were not comparable. In this paper, the wear volume was utilized for the wear rate calculations of the specimens. Additionally, the wear volume can be calculated through the wear track profile. The specific wear rate equation was as follows:

$$K = V/PS \quad (1)$$

where  $K$  is the specific wear rate ( $\text{mm}^3 \text{N}^{-1} \text{m}^{-1}$ ),  $V$  is the wear volume ( $\text{mm}^3$ ),  $P$  is a load (N), and  $S$  is the total sliding distance (m) [17].

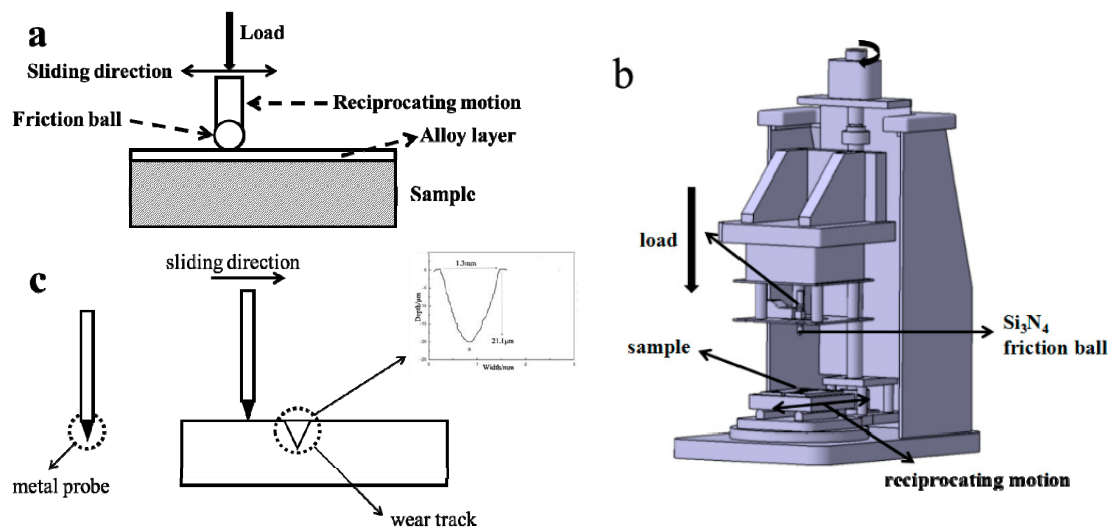


**Figure 3.** The schematic diagram of reciprocating friction (a), the equipment drawing of CET-I friction-wear tester (b) and the schematic diagram of profilometer equipped by the friction-wear tester (c).

## 3. Results and Discussion

### 3.1. Microstructures of Chromizing Coating

The surface morphology and chemical composition of the chromizing coating are presented in Figure 4a,b. It exhibited compact and uniform structure without porosity or cracks. The chromizing coating contained mainly Cr (55.87 wt.%) and Fe (36.23 wt.%). From the composition distribution (Figure 5b), it could be found that the number of Fe element increased gradually within the range of 6~7  $\mu\text{m}$ , indicating that the Fe had diffused towards the coating. According to the iron-carbon phase diagram, both Fe and Cr could be indefinitely dissolved. Combined with the XRD pattern and EDS results, it could be inferred that these two elements existed within the chromizing coating in the form

of a [Fe,Cr] solid solution. The XRD pattern (Figure 4c) showed that the chromizing coating consist of [Fe,Cr], Cr, Cr<sub>23</sub>C<sub>6</sub>, and Cr<sub>7</sub>C<sub>3</sub>. High hardness chromium carbide (Cr<sub>23</sub>C<sub>6</sub> and Cr<sub>7</sub>C<sub>3</sub>) can effectively improve the hardness of metallic card clothing.

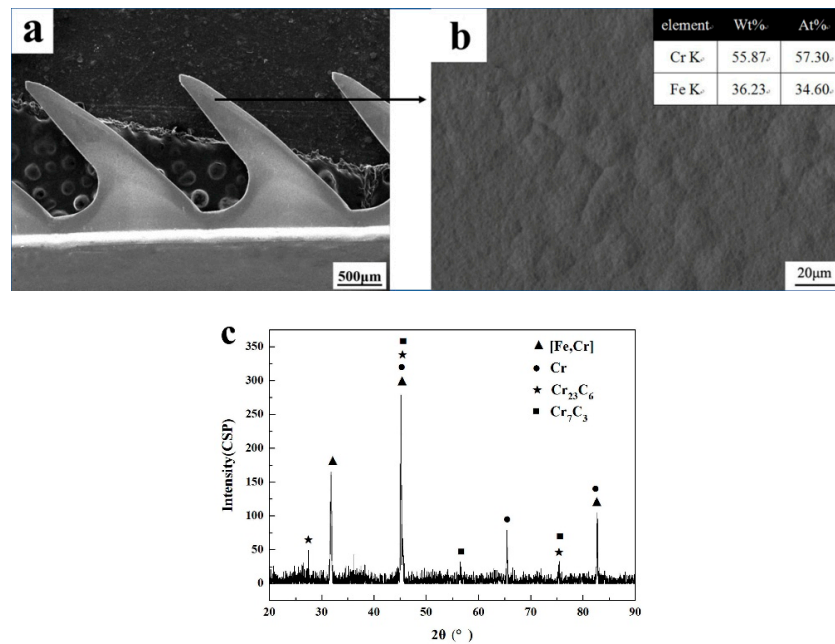


Figure 4. Surface morphologies (a,b) and XRD (X-ray diffraction method) patterns (c) of chromizing coating.

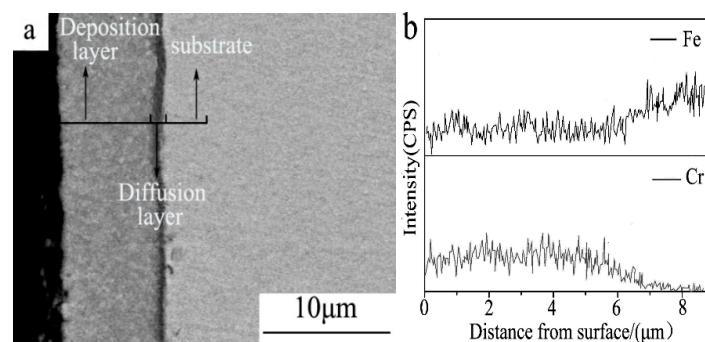


Figure 5. Cross-sectional microstructure (SEM) and composition distribution (EDS) of chromizing coating. (a) cross-sectional microstructure; (b) composition distribution

The cross-sectional microstructure (SEM) and composition distribution (EDS) of chromizing coating are presented in Figure 5a. It exhibited a layered distribution without defects such as porosity, cracks or impurities. The cross-sectional microstructure of the chromizing coating (Figure 5a) was mainly consisting of the deposition layer, diffusion layer and the substrate. From the composition distribution of the chromizing coating presented in Figure 5b, it can be seen that the diffusion of Cr and Fe is obvious which implied the characteristic of metallurgical bonding between the coating and substrate. This structure could effectively improve the adhesion between the coating and the substrate. From the composition distribution it could be observed that the thickness of the deposited layer was approximately 6 µm and the diffusion layer thickness was approximately 1 µm.

### 3.2. Microhardness Test

The results of microhardness test for the metallic card clothing before and after plasma surface alloying were presented in Table 3. It can be seen that there were difference in the hardness of metallic card clothing at different positions. After surface treatment with double glow technology, the hardness

difference of all parts of metallic card clothing increased, and the average value of hardness was 564.9 HV<sub>0.05</sub>, which was approximately 1.55 times the metallic card clothing hardness value.

**Table 3.** Results of microhardness test for the metallic card clothing before and after plasma surface alloying (HV<sub>0.05</sub>).

Sample	Test Point	1	2	3	4	5	Average Value
The Metallic Card Clothing	a	451.3	458.7	462.8	478.1	476.6	475.5
	b	328.2	352.6	334.2	320.5	324.8	342.8
	c	301.1	319.4	324.2	318.3	326.4	317.9
After Plasma Surface Alloying	a	549.3	552.8	574.5	569.7	577.7	564.8
	b	546.8	567.9	553.6	584.5	566.8	564.3
	c	576.9	556.3	546.5	578.5	570.4	565.7

### 3.3. Nanoindentation Tests

The wear resistance of materials always depends on the material hardness. Consequently, a high hardness could effectively improve the wear resistance of materials [18]. In recent years, some researchers considered that the hardness and elastic modulus ratio also constitutes a parameter for the material wear resistance measurements. The H/E was the resistance of elastic strain to failure and the H<sup>3</sup>/E<sup>2</sup> represented the resistance to plastic deformation of the material [19]. A high H/E could improve the wear resistance and the fatigue resistance [20].

Force-depth curves of uncoated and coated samples are shown in Figure 6a. The results of nanoindentation testing demonstrated that the coating had a significant effect on the mechanical properties of metallic card clothing. The nanohardness and elastic modulus could be calculated through the force-depth curves and the Oliver-Pharr method [13,15]. Additionally, the results are presented in Figure 6b. The nanohardness (H) value of the metallic card clothing was 3.41 GPa; the nanohardness (H) value of the chromizing coating was 6.36 GPa, which was approximately 1.87 times the metallic card clothing nanohardness value. The elastic modulus (E) of the metallic card clothing was 161 GPa and the elastic modulus (E) of the chromizing coating was 118 GPa, which was lower compared to the metallic card clothing. Due to the ion sputtering effect, the deposition layer could be divided into the external gassy surface layer and the internal compact texture layer [8]. The external gassy surface layer of the deposition layer surface led to the lower elastic modulus of the chromizing coating compared to the metallic card clothing. The H/E ratios of the metallic card clothing, and the chromizing coating were  $2.12 \times 10^{-2}$  and  $5.38 \times 10^{-2}$ , respectively. The H<sup>3</sup>/E<sup>2</sup> ratios of the metallic card clothing and the chromizing coating were  $1.53 \times 10^{-3}$  and  $1.85 \times 10^{-2}$ .

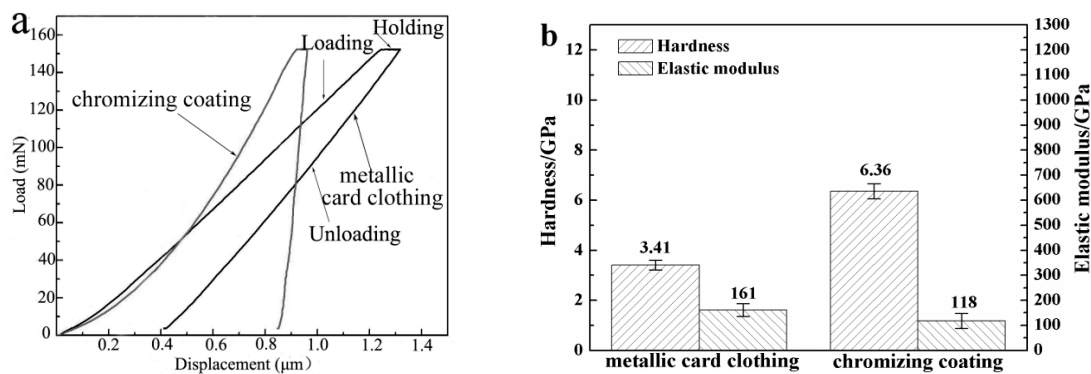


**Figure 6.** Nano indentation curve, nanohardness and elastic modulus bar graph of the metallic card clothing before and after plasma surface alloying. (a) Force-depth curves of uncoated and coated samples, and (b) hardness and elastic modulus of uncoated and coated samples.

### 3.4. Sliding Friction Behaviors of the Metallic Card Clothing Before and After Plasma Surface Alloying under Various Sliding Speeds at Room Temperature

The friction coefficients versus the sliding distances of the metallic card clothing before and after plasma surface alloying under various sliding speeds are presented in Figure 7a–c. The friction coefficient fluctuation improved with the sliding speed increase. The heat generated during friction was the reason for the changes of organization, structure, roughness of surface with the sliding speed increasing, which accordingly led to changes of the friction coefficient [21]. Figure 7d presents the friction coefficient variation curve of the samples along with sliding speeds. The friction coefficients of the chromizing coating decreased first and consequently increased as the sliding speed increased. When the sliding speed was 4 m/min, the chromizing coating presented the lowest friction coefficient. When the sliding speed was 4 m/min, the friction coefficient curve slope of the metallic card clothing changed. Therefore, as the sliding speed increased, the friction coefficient of the metallic card clothing gradually increased. The significantly lower friction coefficients of the chromizing coating demonstrated that the alloy layers were effective in the tribological properties improvement [22].

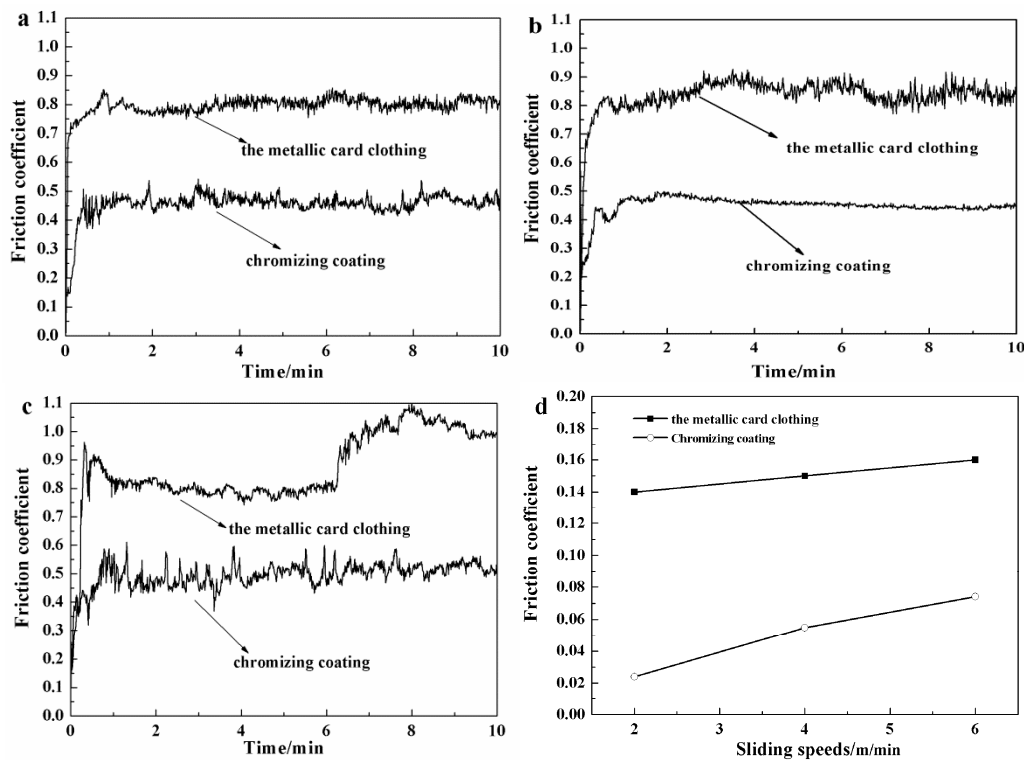


**Figure 7.** Friction coefficient vs. sliding time for untreated and treated samples under various sliding speeds: (a) 2 m/min, 420 g; (b) 4 m/min, 420 g; (c) 6 m/min, 420 g; and (d) variation tendency of friction coefficient.

The wear profiles of the metallic card clothing before and after plasma surface alloying under various sliding speeds are presented in Figure 8. Figure 8d presents the wear volume variation curve of the samples along with sliding speeds. The wear volume increased along with the sliding speeds. It's remarkable that the chromizing coating wear slowed down, when the sliding speed exceeded 4 m/min. The specific wear rates of the metallic card clothing before and after plasma surface alloying at different sliding speeds are presented in Table 4. It was apparent that the specific wear rate of the chromizing coating with low fluctuation was significantly lower compared to metallic card clothing under various sliding speeds. This indicated the excellent wear resistance of the coating. The lower wear rate of the chromizing coating was attributed to the high  $H/E$  and  $H^3/E^2$  ratios.

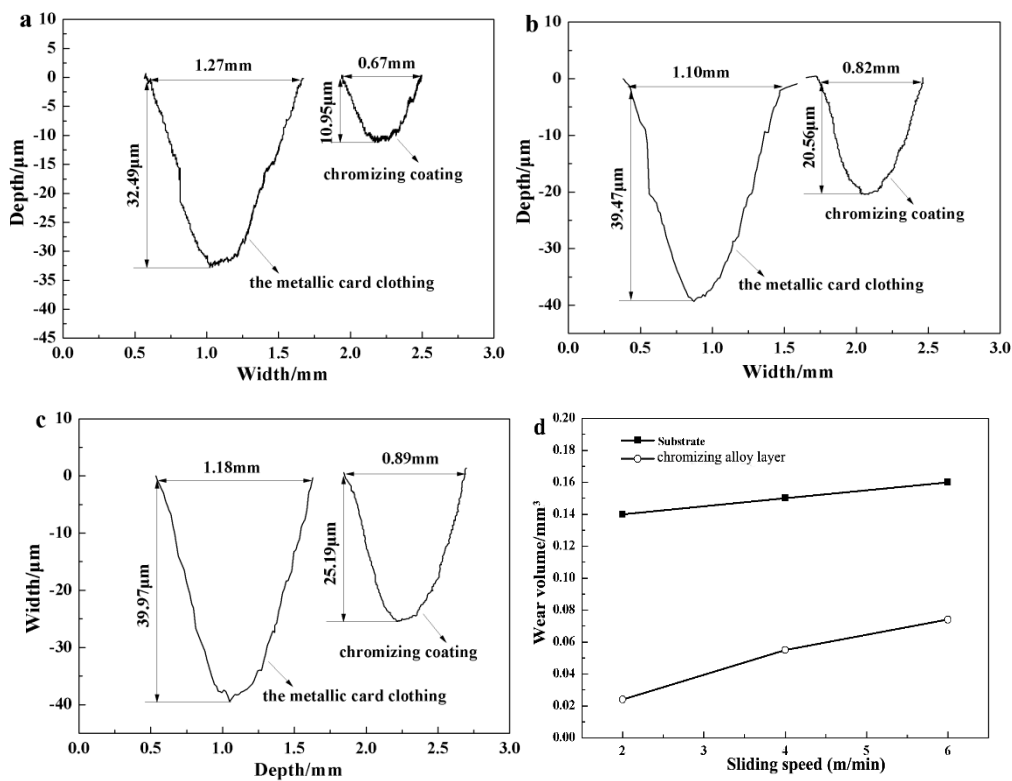


**Figure 8.** Wear profiles for uncoated and coated samples under various speeds: (a) 2 m/min; (b) 4 m/min; (c) 6 m/min; and (d) variation tendency of wear profile.

**Table 4.** Specific wear rate under various sliding speeds for the metallic card clothing before and after plasma surface alloying.

Load (g)	Sliding Speed (m/min)	Specific Wear Rate ( $10^{-4} \cdot \text{mm}^3 \cdot \text{N}^{-1} \cdot \text{m}^{-1}$ )	
		Metallic Card Clothing	Chromizing Coating
420	2	16.38	2.91
	4	9.06	3.30
	6	6.26	2.95

As the sliding speed increased, the wear mechanisms of the steel, the aluminum alloys and other aluminum foundation composite materials would also change [23]. Figure 9 presents the wear track morphology of the chromizing coating at various sliding speeds. When the sliding speed was 2 m/min, only slight scratches existed on the wear track surface, while the alloy layer mainly presented adhesive wear. When the sliding speed increased to 4 m/min, the fast friction produced a thermal effect. As the sliding velocity increased, the friction pair interface shear stress increased [24]. Under the shear stress action, the wear debris as well as a high amount of scratches appeared on the wear track surface, while the wear mechanism was converted to abrasive wear. As the sliding speed continued to increase, the shear pressure became high and the coating was flaked. The friction mechanism was mainly abrasive wear. A large amount of scratches could be observed in Figure 9c. Moreover, the adhesion film could be observed near the edge of the wear track. The good bonding strength between the deposition layer and the diffusion layer prevented delamination of the deposited layer during friction. The deformed deposition layer acted as a soft film lubricant, subsequently reducing both the friction coefficient and specific wear rate. When the sliding speed was 2 m/min, the wear mechanism of the chromizing coating was abrasive wear. Moreover, the wear mechanism gradually changed from adhesive wear to abrasive wear as the sliding velocity increased (4–6 m/min). It could be observed from Figure 8d that

when the sliding speed exceeded 4 m/min, the wear volume growth rate of the chromizing coating changed, which might be due to the change of the wear mechanism.

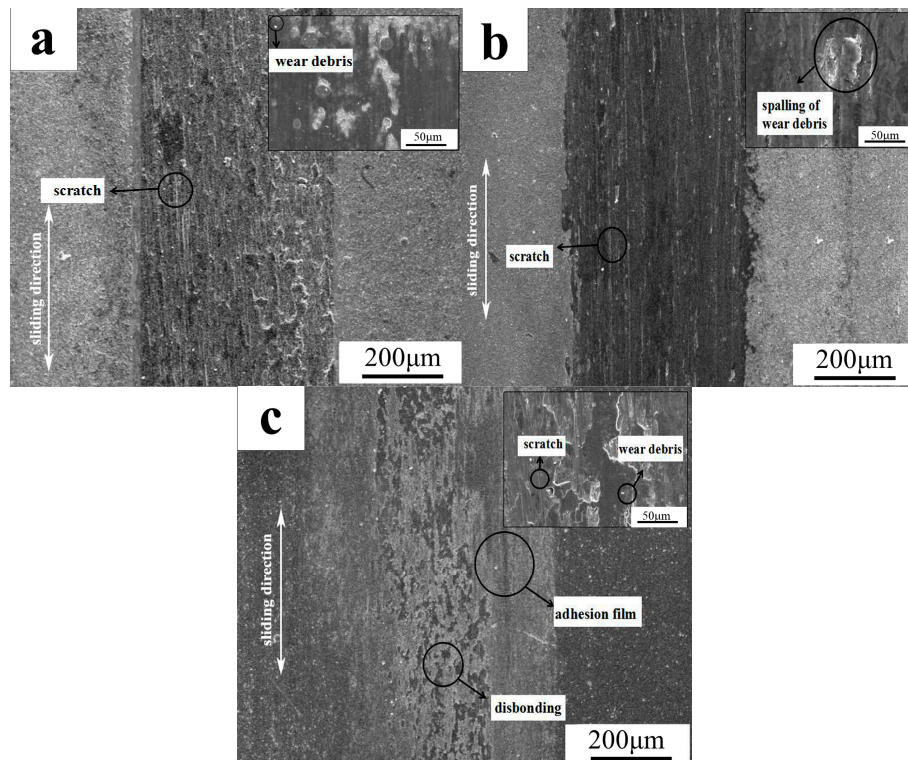


**Figure 9.** Wear track morphology of chromizing coating under various sliding speeds (a) 2 m/min; (b) 4 m/min; and (c) 6 m/min.

#### 4. Conclusions

In this work, we report a new surface strengthening process (double glow technology) to improve the wear resistance of the metallic card clothing. The chromizing coating was successfully prepared on the metallic card clothing through the double glow technology. The surface morphologies, microstructure, and phase composition were characterized by scanning electron microscopy (SEM), energy dispersive spectroscopy (EDS), and X-ray diffraction (XRD) method. The hardness was examined by Vickers hardness test and nano-indentation test. The effects of different sliding speeds on the friction properties of metallic card clothing were studied. The following conclusions can be drawn from this study.

(1) The surface of the chromizing coating is smoother without granular sediment. The bond between the chromizing coating and metallic card clothing was metallurgical, which guarantees high adhesion between coating and metallic card clothing. The whole thickness of coating was approximately 7  $\mu\text{m}$ .

(2) The hardness of metallic card clothing increased obviously after plasma surface alloying. The average value of hardness was 564.9  $\text{HV}_{0.05}$ , which was approximately 1.55 times the metallic card clothing hardness value. The  $H/E$  ratio and the  $H^3/E^2$  ratio of the chromizing coating were approximately 2.5 times and 12 times the metallic card clothing ratios, which account for the significantly lower specific wear rate of chromizing coating compared to the metallic card clothing.

(3) The wear resistance of metallic card clothing was obviously improved after strengthening by double glow technology. The specific wear rates of metallic card clothing after plasma surface chromizing were 2.91, 3.30, and  $2.95 \times 10^{-4} \cdot \text{mm}^3 \cdot \text{N}^{-1} \cdot \text{m}^{-1}$ , which was significantly lower than the wear rate of metallic card clothing before plasma surface chromizing.

(4) Double glow plasma surface metallurgy technology is easy to operate, stable in process parameters and suitable for mass production of metal card clothing. The chromizing coating processed by the double glow technology provides a solution to strengthening the wear resistance of the metal card clothing.

**Author Contributions:** Conceptualization: D.W., F.L.; Methodology: S.L. and X.C.; Data curation, D.W., P.Z., Z.W.; Formal analysis, F.L.; Investigation, S.L.; Methodology, S.L., X.C.; Software, F.D; writing—original draft preparation, D.W.; writing—review and editing, D.W., F.L.

**Funding:** This project was supported by Natural Science Foundation for Excellent Young Scientists of Jiangsu Province, China (Grant No. BK20180068), China Postdoctoral Science Foundation funded project (Grant No. 2018M630555), the Fundamental Research Funds for the Central Universities, China (Grant No. NS2018039), Opening Project of Key Laboratory of Materials Preparation and Protection for Harsh Environment (Nanjing University of Aeronautics and Astronautics), Ministry of Industry and Information Technology (Grant No. NJ2018009), Opening Project of Jiangsu Key Laboratory of Advanced Structural Materials and Application Technology (Grant No. ASMA201701).

**Conflicts of Interest:** The authors declare no conflict of interest.

## References

1. Wu, L.; Wang, W.; Ni, H. A View on Wear Mechanism of Metallic Card Clothing. *J. Donghua Univ.* **2008**, *25*, 324–327.
2. Chen, Y. Wear and control of MCC for the carding machine. *Text. Accessories* **2017**, *44*, 290–295.
3. Zhu, W.; Chen, R. Wear characteristics of metallic clothing. *J. Iron. Steel Res.* **1992**, *4*, 49–54.
4. Xu, Z.; Liu, X.; Zhang, P.; Zhang, Y.; Zhang, G.; He, Z. Double glow plasma surface alloying and plasma nitriding. *Surf. Coat. Technol.* **2007**, *201*, 4822–4825. [[CrossRef](#)]
5. Survilienė, S.; Jasulaitienė, V.; Češūnienė, A.; Lisowska-Oleksiak, A. The use of XPS for study of the surface layers of Cr–Co alloy electrodeposited from Cr(III) formate-urea baths. *Solid State Ionics* **2008**, *179*, 222–227. [[CrossRef](#)]
6. Liu, Y.; Zhang, P.; Wei, D.; Wei, X.; Chen, X.; Ding, F. Corrosion behavior of tantalum alloying on  $\gamma$ -TiAl by double-glow plasma surface metallurgy technique. *Surf. Interface Anal.* **2017**, *49*, 674–681. [[CrossRef](#)]
7. Chen, Z.; Wu, W.; Cong, X. Oxidation Resistance Coatings of Ir–Zr and Ir by Double Glow Plasma. *J. Mater. Sci. Technol.* **2014**, *30*, 268–274. [[CrossRef](#)]
8. Wei, D.-B.; Zhang, P.-Z.; Yao, Z.-J.; Liang, W.-P.; Miao, Q.; Xu, Z. Oxidation of double-glow plasma chromising coating on TC<sub>4</sub> titanium alloys. *Corros. Sci.* **2013**, *66*, 43–50. [[CrossRef](#)]
9. Xu, J.; Liu, Y.; Wang, J.; Kui, X.; Gao, Y.; Xu, Z. A study on double glow plasma surface metallurgy Mo–Cr high speed steel of carbon steel. *Surf. Coat. Technol.* **2007**, *201*, 5093–5096. [[CrossRef](#)]
10. Qin, L.; Tian, L.; Fan, A.; Tang, B.; Xu, Z. Fatigue behavior of surface modified Ti–6Al–4V alloy by double glow discharge plasma alloying. *Surf. Coat. Technol.* **2007**, *201*, 5282–5285. [[CrossRef](#)]
11. Zhang, P.; Xu, Z.; Zhang, G.; He, Z. Surface plasma chromized burn-resistant titanium alloy. *Surf. Coat. Technol.* **2007**, *201*, 4884–4887. [[CrossRef](#)]
12. Qiu, Z.-K.; Zhang, P.-Z.; Wei, D.-B.; Wei, X.-F.; Chen, X.-H. A study on tribological behavior of double-glow plasma surface alloying W–Mo coating on gear steel. *Surf. Coat. Technol.* **2015**, *278*, 92–98. [[CrossRef](#)]
13. Cong, W.; Yao, Z.; Zhu, X. Sliding wear of low carbon steel modified by double-glow plasma surface alloying with nickel and chromium at various temperatures. *Wear* **2010**, *268*, 790–796. [[CrossRef](#)]
14. Wei, D.-B.; Zhang, P.-Z.; Yao, Z.-J.; Wei, X.-F.; Zhou, J.-T.; Chen, X.-H. Oxidation behaviour of plasma surface alloying on Ti<sub>6</sub>Al<sub>4</sub>V alloy. *Surf. Eng.* **2016**, *34*. [[CrossRef](#)]
15. Oliver, W.C.; Pharr, G.M. An Improved Technique for Determining Hardness and Elastic Modulus Using Load and Displacement Sensing Indentation experiments. *J. Mater. Res.* **1992**, *7*, 1564–1583. [[CrossRef](#)]
16. American Society for Testing and Materials. Standard Test Method for Linearly Reciprocating Ball-on-Flat Sliding Wear. Philadelphia, PA, USA, 2005. Available online: <https://www.astm.org/Standards/G133.htm> (accessed on 3 April 2019). [[CrossRef](#)]
17. Qiu, Z.; Zhang, P.; Wei, D.; Duan, B.; Zhou, P. Tribological behavior of CrCoNiAlTiY coating synthesized by double-glow plasma surface alloying technique. *Tribol. Int.* **2015**, *192*, 512–518. [[CrossRef](#)]

18. Tillmann, W.; Vogli, E.; Hoffmann, F.; Kemdem, P. Influence of Substrate Nitriding on Adhesion, Friction and Wear Resistance of DLC (Diamond-Like Carbon)-Coatings. *Key Eng. Mater.* **2010**, *438*, 211–218. [[CrossRef](#)]
19. Leyland, A.; Matthew, A. On the Significance of the H/E Ratio in Wear Control: A Nanocomposite Coating Approach to Optimized Tribological Behavior. *Wear* **2000**, *246*, 1–11. [[CrossRef](#)]
20. Zeng, Z.; Zhou, Y.; Zhang, B.; Sun, Y.; Zhang, J. Designed fabrication of hard Cr-Cr<sub>2</sub>O<sub>3</sub>-Cr<sub>7</sub>C<sub>3</sub>, nanocomposite coatings for anti-wear application. *Acta Mater.* **2009**, *57*, 5342–5347. [[CrossRef](#)]
21. Zhou, F.; Wang, X.; Adachi, K.; Kato, K. Influence of normal load and sliding speed on the tribological property of amorphous carbon nitride coatings sliding against Si<sub>3</sub>N<sub>4</sub> balls in water. *Surf. Coat. Technol.* **2008**, *202*, 3519–3528. [[CrossRef](#)]
22. Yu, L.; Huang, T.; Xu, J. Microstructure, mechanical and tribological properties of TaCN composite films. *Surf. Eng.* **2014**, *33*, 1–6. [[CrossRef](#)]
23. Straffelini, G.; Molinari, A. Dry sliding wear of Ti-6Al-4V alloy as influenced by the counterface and sliding conditions. *Wear* **1999**, *236*, 328–338. [[CrossRef](#)]
24. Zhong, M.; Liu, W.; Zhang, H. Corrosion and wear resistance characteristics of NiCr coating by laser alloying with powder feeding on grey iron liner. *Wear* **2006**, *260*, 1349–1355. [[CrossRef](#)]



© 2019 by the authors. Licensee MDPI, Basel, Switzerland. This article is an open access article distributed under the terms and conditions of the Creative Commons Attribution (CC BY) license (<http://creativecommons.org/licenses/by/4.0/>).